

Accepted Manuscript

Fracture mechanics based estimation of fatigue lives of laser welded joints

Rakesh Goyal, Sergey Bogdanov, Mohamad El-zein, Grzegorz Glinka



PII: S1350-6307(17)31405-X
DOI: [doi:10.1016/j.engfailanal.2018.07.017](https://doi.org/10.1016/j.engfailanal.2018.07.017)
Reference: EFA 3547

To appear in: *Engineering Failure Analysis*

Received date: 28 January 2018
Revised date: 23 June 2018
Accepted date: 20 July 2018

Please cite this article as: Rakesh Goyal, Sergey Bogdanov, Mohamad El-zein, Grzegorz Glinka , Fracture mechanics based estimation of fatigue lives of laser welded joints. Efa (2018), doi:[10.1016/j.engfailanal.2018.07.017](https://doi.org/10.1016/j.engfailanal.2018.07.017)

This is a PDF file of an unedited manuscript that has been accepted for publication. As a service to our customers we are providing this early version of the manuscript. The manuscript will undergo copyediting, typesetting, and review of the resulting proof before it is published in its final form. Please note that during the production process errors may be discovered which could affect the content, and all legal disclaimers that apply to the journal pertain.

Fracture mechanics based estimation of fatigue lives of laser welded joints

Rakesh Goyal¹, Sergey Bogdanov², Mohamad El-zein³ and Grzegorz Glinka²

¹John Deere Asia Technology Innovation Center, Pune, MH 411013, India

GoyalRakesh@JohnDeere.Com

²Mechanical and Mechatronics Engineering, University of Waterloo, Waterloo, ON, Canada

³Deere & Company, MTIC, One John Deere Place, Moline, IL 61265, Unites States

ABSTRACT

The conventional joining methods like resistance spot welding and arc welding have several challenges during joining of thin sheets of high strength steel materials. One of the main challenge is that application of these joining methods may result in a severe distortion of welded structure. Therefore laser welding process has emerged as an alternative joining process which can help mitigate some of these challenges. Lower heat input from laser during the welding process results in a smaller size weld heat affected zone and also in lower overall distortion of the structure. The laser welding process presents an exciting opportunity in designing lighter weight structures. However, the major roadblock to application of laser welding method for large structural parts is that fatigue behavior of laser welded joints is not yet well understood. In order to study the fatigue performance of laser welded joints, detailed experimental and numerical investigations have been carried out and the results are presented in this work. The scope of experimental studies included a large set of coupons with different thicknesses and material combinations. Experimental fatigue test data has been generated for the laser welded joints produced using thin sheets of three grades of high strength steel materials (HSLA and UHSS grades) of several thicknesses (1mm, 1.6mm, 2mm and 3mm). The fatigue test data sets were obtained at R-ratios of R=0.1, R=0.2 and R=0.3. Another variable introduced into experimental studies was an orientation of laser weld joint with respect to applied loading direction. After fatigue tests were completed, detailed metallurgical investigations have been carried out to understand the failure mechanism and the crack growth behavior in laser welded joints. Based on the observed experimental and numerical studies it was concluded that the strain life based fatigue analysis method which has been successfully applied to study weld toe failures for the arc weld joints is not sufficient for the evaluation of laser welded joints. This is due to the reason that laser welded joints have unique challenges due to weld root crack failures and extremely high stress concentration at the location of crack initiation in the root of laser welded joints between the plates. The fracture mechanics based method has been developed for the fatigue life assessment of laser welded joints. In order to apply this method comprehensive three dimensional finite element studies were performed. Numerical studies show good correlation of the estimated fatigue lives obtained using proposed fracture mechanics method with the experimental data.

Key Words: Laser welds, Stress analysis, Fracture Mechanics, High Strength steels, Fatigue Life

1. Introduction

The need for light weighting of structural parts in the automotive and other ground vehicles machinery is increasing than ever mainly due to emission control regulations and fuel efficiency requirements. The use of high strength steel materials along with thinner gauge sections is one of the ways to save weight and increase fuel efficiency. It is also well known that various types of joints are integral to any structure. Conventional joining methods such as gas metal arc welding and resistance spot welding are widely used across the industry for joining structural members. In addition to good understanding of the manufacturing process variables, significant amount of design data and level of confidence exist with the design and analysis methods of joints produced using these contemporary conventional processes. Laser welding on the other hand is an emerging technology which has been utilized for few years by the automotive industry but the widespread usage of it is still limited especially in the case of manufacturing of heavily loaded structural components. The laser welding process has shown great potential for the improved manufacturability of such assemblies especially when joining thin sheets of high strength steel grades. Due to much lower heat input of the laser welding process, it results into minimal distortion of large welded assemblies, which can greatly help to achieve and maintain tighter dimensional tolerances.

Laser welding enables to easily join two plates of sheet metal, however such a joint introduces, between the two welded plates, a crack-like stress concentration region which can significantly influence the fatigue life of the joint. Unfortunately, the understanding of fatigue performance of laser welded structural joints is rather limited. Therefore the failure mechanism of laser welded joints under cyclic loading conditions needs to be better understood [1-3]. A significant gap exists in terms of the design and analysis methods when using laser welded joints in cyclically loaded structural components [4-5]. Strain life based fatigue analysis method commonly used for analyzing arc welded joints are not suitable for the design of laser welded joints. Therefore the finite element stress analysis (FEA) and fatigue analysis methods for evaluating laser welded joints need to be developed to help accelerate the product design cycle and improve the level of confidence while designing with these joints.

In order to address the above gaps, the present research is focused on the development of a methodology to predict fatigue life of laser welded joints. Various aspects of the methodology are discussed in the paper. Detailed description of the experimental work along with summary of experimental findings has been discussed in the paper. The challenges related to applicability of strain life method for the analysis of laser welded joints have been highlighted. The details of numerical analysis including 3D fine mesh FE modeling of laser welded joint have been presented as well. The fracture mechanics based method has been applied to estimate fatigue life of laser welded joints and the results

have been compared against the experimentally obtained data. Conclusions and recommendations based on the results presented earlier are discussed at the end of the paper.

2. Materials

Three different grades of high strength steel material have been used in the investigation presented below. High strength low alloy steel grades (HSLA-50 and HSLA-80) and ultra-high strength steel grade (UHSS-100) have been utilized during this work. The chemical composition and mechanical properties of these high strength steel materials are shown in Table 1 and 2 respectively. For each of these 3 material grades, cyclic stress-strain curves and Manson-Coffin curves were obtained experimentally and are shown in Fig. 1.

3. Experimental investigation

Single lap joints were manufactured using the seam stepper laser welding process. All specimens were joined by a laser weld of 20mm long and 2mm wide. Each welded plate was 120mm long and 38 mm wide. The overlap length between the two plates was 36mm. The spacer tabs of 50mm each were resistance spot welded on each side. This was done in order to minimize the specimen deflection due to testing grip alignment errors. The thickness of spacer tabs was selected so that the neutral axis passed through middle of a plate (the thinner plate in the case of dissimilar plate thicknesses) as shown in Fig. 2. The spacer tabs were spot welded to each plate before the laser welding of the two plates was performed. The laser welding process parameters were optimized so as to achieve at least 1mm of penetration through the bottom plate of the lap joint. The laser welds were made with 3 different weld orientations with respect to the loading direction and designated as 0° welds (weld length parallel to loading direction), 45° welds (weld length oriented at 45° to the loading direction) and 90° welds (welds length perpendicular to the loading direction), as shown in Fig. 3. In total 56 lap joint samples were manufactured and tested for evaluating the fatigue performance of laser weld joints.

The fatigue testing was performed using 100kN load frame servo-hydraulic testing machine at room temperature of 25°C and relative humidity of 55% RH. All of the fatigue experiments were performed using constant amplitude loading and mostly performed at 2 different stress ratios i.e. $R=0.1$ and $R=0.3$ and the frequency range of 3-5Hz. A few specimens were also tested at $R=0.2$. All of the specimens were tested until complete fracture of the joint. The summary of all experimentally tested samples is shown in Table 3. Detailed metallurgical analysis of failed samples was carried out to understand the fracture behavior of laser welded joints under cyclic loading conditions.

4. Fatigue life analysis methodology

There are three most commonly used methods for evaluating fatigue life of a structure: the stress life based method, the strain life based method and the method based on the linear elastic fracture mechanics (LEFM). The stress life method is the oldest one but it is still the most widely used method for the assessment of number of fatigue cycles to failure in practice. This method is simple and easy to use, although limited in many capabilities e.g. it doesn't work well with variable amplitude load histories. Similar to arc welded joints, several variations of the stress life methods such as structural stress, hot spot stress and local stress method [6-11] have been explored for the fatigue life assessment laser welded joints assuming various notch reference radii. The main difficulty with the stress life method is the identification of the reference nominal stress for correlating it with the number of cycles to fatigue failure in a complex structure with multiple and mixed modes of loading. The strain life method requires sufficiently accurate evaluation of actual stresses and strains at the critical notch location such as at the weld root in the case of a laser weld joint, which makes it less robust method because it must account for the local notch geometry. Implementation of the strain life methodology requires information of the 'notch effect' or the stress concentration around the weld nugget periphery to estimate the crack initiation life. The actual stress effect resulting from the stress concentration near the weld nugget is not sufficiently well understood, in the case of laser weld joints [12]. Earlier work [13-15] as well as the studies performed during this work have shown that there is extremely high stress concentration at the root of a laser weld joint and the crack initiation life could be relatively short. Therefore it makes it difficult to apply the strain life approach but also it suggests that the major portion of the total fatigue life is dominated by crack propagation.

4.1 Fracture mechanics based fatigue life analysis

The fatigue crack growth (FCG) method enables fatigue life prediction for the variable amplitude loading histories but involves higher levels of complexity because detailed knowledge of the stress field distribution along potential crack path is needed. The main advantage of an analysis based on the LEFM approach is that it allows to model more realistically the entire fatigue process rather than simply using an empirical correlation between number of applied cycles and applied stress or strain amplitude. The FCG method requires detail evaluation of stress distribution in a plane of interest and fatigue crack growth material properties. The use of fracture mechanics method for the fatigue life estimation of laser welded joints has been advocated by several authors [16 -18]. One of the major challenges with the conventional LEFM approach is that the initial crack size is needed as the input, which is difficult to obtain experimentally. The UniGrow FCG model based on total fatigue life approach [19-21] has been utilized in this work which requires among others a material characteristic property, ρ^* as input rather than the initial crack size. As per the total fatigue life approach the entire fatigue life can be estimated using

LEFM with a crack propagation from its initial crack size of ρ^* to the final fracture, thus avoiding the need to separately estimate the fatigue crack initiation and propagation life. The UniGrow FCG model based approach has been successfully applied for the fatigue life assessment of arc welded joints [22] but this is the first attempt to apply this approach for the laser welded joints. The laser welded joints pose additional challenges as compared to arc welded joints [23] with the main difference being failure mechanism of these joints under cyclic loading conditions.

4.2 The UniGrow fatigue crack growth model

As per the UniGrow FCG model, the crack is modeled as a blunt notch with finite tip radius ρ^* . The Fatigue crack growth is regarded as successive crack increments (re-initiation) over the distance ρ^* , see Fig. 4. The number of cycles N^* necessary to break the material over the distance ρ^* can be determined from the cyclic curve (Ramberg-Osgood) and strain life fatigue material curve (Manson-Coffin) obtained experimentally from smooth specimens. The instantaneous fatigue crack growth rate can be determined as:

$$da/dN = \rho^*/N^* \quad (1)$$

The UniGrow fatigue crack growth model uses the total driving force $\Delta\kappa$, Eq. (2) and a set of memory rules to account for the loading sequence effects. The detailed description of the memory rules was given by Mikheevskiy in reference [24]. Contrary to the crack tip closure-based fatigue crack growth models, the UniGrow model uses the residual stress distribution created due to local reversed plastic deformations (Fig. 4) created around the crack tip. According to the UniGrow model, these residual stresses left in the plastically deformed region behind the crack tip needs to be transformed into the residual stress intensity factor (SIF), K_r . This parameter is then used to calculate the total driving force, $\Delta\kappa$ along with the applied stress intensity factor range, ΔK and the maximum applied stress intensity factor, K_{max} , Eq. (2). The total driving force, $\Delta\kappa$ is subsequently related, Eq. (3), to the fatigue crack growth rate da/dN .

$$\Delta\kappa = (\Delta K + K_r)^{1-p} (K_{max} + K_r)^p \quad (2)$$

$$da/dN = C \cdot (\Delta\kappa)^\gamma \quad (3)$$

Parameters C , γ , and p can be found from the Manson-Coffin and Ramberg-Osgood material properties or the experimentally generated fatigue crack growth data. The fatigue crack growth analysis model requires a certain amount of basic experimental constant amplitude fatigue crack growth material data. The raw fatigue crack growth data sets are obtained in the form of the “a vs. N” relationship, then transformed into ΔK vs da/dN relationship and finally this data is corrected for R ratio and plasticity effects by using Willenborg [6], Wheeler [25], closure [26] or UniGrow [27] model. The main advantage of the UniGrow

model comes from the fact that it is derived from the strain-life material properties and limited fatigue crack growth data. As the experimental fatigue crack growth data was not available in this particular case, the necessary UniGrow material property parameters were obtained using equations proposed by Noroozi and Glinka [19] and based on the published data [28-29] obtained from smooth specimens as shown in Table 4.

One of the critical steps in the FCG analysis procedure is regarding the choice of an initial crack shape model. Two potential geometries were considered: the quarter elliptical corner crack and the semi-elliptical crack. Observation of specimen fractured surfaces (Fig. 5) have revealed that the initial crack is closer to a semi-elliptical shape.

There are several stress intensity factor (SIF) solutions available for various modes of loading for semi-elliptical crack but none of them can be used in the case (Fig. 5) being discussed. In order to overcome limitations of ready-made SIFs it was proposed to evaluate the SIF by using the weight function method. Originally proposed by Bueckner [30] and Rice [31], the weight function method is based on the principle of superposition. The stress intensity factor for a cracked body subjected to an external loading, S , (Fig. 6a) can be obtained by determining the stress intensity factor in a geometrically identical body with the local stress field $\sigma(x)$ applied to the crack faces (Fig. 6c). The local stress field $\sigma(x)$ induced by the external load S in the prospective crack plane should be determined by neglecting the presence of the crack (Figure 6b). Therefore, the stress intensity factor takes a form of the following definite integral, Eq. (4):

$$K = \int_0^a \sigma(x) m(x, a) dx \quad (4)$$

Where $m(x,a)$ is the weight function and $\sigma(x)$ is the stress distribution, induced by the loads in the uncracked body.

4.3 Estimation of relevant stress distributions

The FCG analysis requires a detailed stress distribution along the critical crack plane path. Such a distribution for the complex geometries can be obtained by performing a solid 3D fine mesh finite elements analysis. The first task is to identify the critical location for the fatigue crack initiation. The metallurgical analysis has confirmed that the location of a crack initiation is the same as the location with highest magnitude of the maximum principal stress obtained from detailed finite element analysis. The critical locations for each of the three different weld orientation were identified as shown in the Fig. 7.

The FE model preparation to capture the effect of micro geometric features such as the weld root radius and the weld geometry with thin sheets using the 3D fine mesh elements involves significant level of complexity. This becomes even more challenging with the addition of variables such as weld orientation, gap between plates, plate thicknesses, loading and boundary conditions. For the laser welded lap joint configuration, it is best to apply displacement rather than load as the controlled input parameter because the controlled displacement ensures parallel motion of the plate and as such it closely adheres to the experimental setup. The end of one of the plate (thick plate in the case of dissimilar thicknesses) was fixed in the sense of all degrees of freedom. At the end of the other plate (the thin plate in the case of dissimilar thicknesses) the uniform displacement field 'u_y' was applied (Figs. 2, 3, 5 and 8). In the case of laser weld joint configurations with 0° and 90° weld orientations only half of the geometry was modelled in the FE analysis due the symmetry of the joint. The measured radius at the root of several laser welded joints was around 17µm and in order to accurately capture the stress concentration effect, at-least 8 elements (Fig. 9) were used along the notch contour.

5. Results and discussions

In all the tested configurations, the crack propagation occurred either through the plates made of HSLA-80 or UHSS-100 steels. Experimental fatigue lives obtained in due course spread over the range from 1000 and to 2 000 000 cycles. Based on the analysis of fractured surfaces the most probable crack initiation sites have been found and they are denoted in Fig. 10. In the case of laser welded joints with 45° and 90° weld orientation different crack behavior have been observed. For the laser welded joint with 90° weld orientation, the fatigue crack growth occurred first around the weld nugget boundary/periphery after growing in the plate thickness from the initiation point at the weld root i.e. interface of the joining sheets. The fatigue crack in the 0° and 45° weld joints initiated at the point of the highest stress concentration on the weld root line and then they grew (Fig. 7) in the direction normal to the applied load rather than along the weld periphery. Similar failure mechanism has been reported earlier [1] in the case of tension-shear lap joints. The total life of fatigue test specimens with 0° and 45° weld orientation can be divided into two phases (each with roughly equal number of cycles). The first phase is the through the thickness propagation of a semi-elliptical fatigue crack. The second phase is the growth of a through thickness crack in the plate width direction. The second phase can be neglected while estimating the useful life of the joint because from the engineering point of view the through thickness crack penetration can be considered as a failure.

The summary of all experimental fatigue test results is presented in Fig. 11. It can be observed that the stress ratio, R does not have significant influence on fatigue lives of laser welded joints within the investigated range. It is also apparent that specimens with larger plate thicknesses showed relatively

longer fatigue lives when obtained under similar control stress. It is most probably attributed to increased stiffness and reduced local bending stress effect as reported in references [14, 16, and 32]. In addition the hardness variation (Fig. 12) as a function of the distance from the center of the weld has been obtained as well. The hardness distribution suggests that there is no significant softening of the weld HAZ similar to the behavior of arc welded joints for these steel grades. Therefore the base material properties can be used for the fatigue analyses.

Dimensions of laser welds were modeled in the FE analysis based on several macrographs of laser welded joint as those shown in Fig. 9 and Fig. 12. Based on the FE analysis of laser welded joints presented above the through thickness stress distributions (Fig. 13) were obtained in the critical crack plane of each of the 8 configurations listed in Table 2. The normal stress component $\sigma_{yy}(z)$, i.e. normal to crack plane, was extracted from (Figs. 5 and 9) the 3D fine mesh FE analysis.

The simulation of welding process was also carried out to understand the state of thermal induced residual stresses around the root of laser welds. Simulation process parameters were adjusted so as to match the thermal hardness profile obtained from the simulation with the weld macrograph shown in Fig. 14. Initial studies have confirmed that compressive residual stress of about 60MPa in magnitude was present at the weld root, which contradicts the assumption made in reference [13] but it is in agreement with the trend reported in references [33-34]. Although some literature data concerned with experimentally measured residual stress data on the outside surface of laser welded joint [35-38] has been reported, the data on the residual stress state near laser weld roots is yet unavailable.

The commercial software package with the UniGrow model implemented has been utilized to perform the fatigue crack growth life analysis. The fatigue crack growth analysis package uses as the input data, the set of mechanical and FCG material properties listed in Table 2 and Table 4 along with the through thickness stress distributions from Fig. 13. Geometrical configurations of analyzed specimens are listed in Table 3. Comparison of predicted total fatigue lives obtained by using the UniGrow based fracture mechanics based method and the corresponding experimentally obtained fatigue lives for all tested samples is shown in Fig. 15. Shown are also in the same Fig. 15 the upper and lower bounds representing 3X (3 times over or under predictions) over and under predictions of fatigue lives respectively around the perfect prediction line. Majority of the data points fall between the perfect prediction line and the 3X under prediction line, which means that predicted fatigue lives are on the conservative side. One of possible reasons for the systematic under-prediction of fatigue lives is not accounting for the compressive residual stresses which might be present at the weld root. It was found that the data points falling below the 3X lower band belong mostly to samples with the laser weld orientation of 0° and 45° . It is clearly visible in Fig. 16 showing the same data but excluding the data points obtained for laser welds with

orientation at 0° and 45° . The reason of the under prediction of fatigue lives of laser welded joints with 0° and 45° orientation can be partially attributed to the semi-elliptical crack model used in this study, which may not be fully appropriate for the crack growth behavior observed experimentally. As noted earlier, crack growth happened parallel to the weld periphery for the samples with laser weld orientation at 0° and 45° resulting in a non-planer crack front, which violates the basic assumption of semi-elliptical crack model. The other factor could be related to the load shedding. The load shedding effect manifests itself in the redistribution of the load transferred through the cracked cross section, i.e. other parts of the section may take more load than at the beginning of the process when the crack was small. Therefore those effects require further studies and possibly the development of a more complex non-planar crack model. Regarding the data point appearing too close to the 3X over prediction bound as shown in Fig. 16, is most likely associated with the improper manufacturing of the test sample. Based on the fractured surface analysis, it was found that due to poor weld quality pure shear failure occurred through the weld itself rather than the expected crack propagation through the plate.

6. Conclusions

Experimental and numerical analyses have been performed to understand the failure mechanism of laser welded joints and to develop a systematic method for fatigue life evaluations. The location of the fatigue crack initiation point and subsequent crack propagation have been evaluated based on the findings obtained from tests and metallurgical analyses. It was found that depending on the orientation of laser welds cracks may grow in a different way before and after penetrating through the plate thickness. Difficulties in applying the traditional fatigue life prediction methods such as stress life and strain life methods have been highlighted as well. The UniGrow fatigue crack growth model based on the LEM principles has been applied for fatigue life assessment of laser welded joints. One of the fundamental assumption in this model is that the initial crack is of a semi-elliptical (in fact semi-circular) shape and it requires the knowledge of the material characteristic property ρ^* is known. The fracture mechanics based approach utilized in this work requires detailed 3D fine mesh FE output data and has shown reasonable fatigue life predictions for engineering design purpose (mostly on the conservative side). The advantage of using the approach is that the FE stress analysis is carried out only once and for un-cracked component. The material properties used in this analysis above were obtained by using the theoretical/analytical expressions but it is highly recommended to carry out two or three standard FCG tests to generate required material data sets. As far as the future work is concerned additional studies are recommended for a wider range of thicknesses involving specimens with 0° and 45° weld orientation to further improve the methodology.

References

1. M. Inohara, H. Akebono, M. Kato, A. Sugeta, Effects of loading mode on the fatigue behavior of laser welds in automobile mild steel sheet, *Weld World* (2016) 60:535–545
2. N. Farabi, D.L. Chen, Y. Zhou, Fatigue properties of laser welded dual-phase steel joints, *Procedia Engineering* 2 (2010) 835–843
3. N. Farabi, D.L. Chen, J. Lib, Y. Zhou, S.J. Dong, Microstructure and mechanical properties of laser welded DP600 steel joints, *Materials Science and Engineering A* 527 (2010) 1215–1222
4. X. He, Finite Element Analysis of Laser Welding: A State of Art Review, *Materials and Manufacturing Processes*, 27: 1354–1365, 2012
5. W. Xu, D. Westerbaan, S.S. Nayak, D.L. Chen, F. Goodwin, Y. Zhou, Tensile and fatigue properties of fiber laser welded high strength low alloy and DP980 dual-phase steel joints, *Materials and Design* 43 (2013) 373–383
6. C.M. Sonsino, M. Kueppers, M. Eibl, G. Zhang, Fatigue strength of laser beam welded thin steel structures under multiaxial loading, *International Journal of Fatigue* 28 (2006) 657–662
7. M. Stoschka, M. Thaler, H. Huemer, W. Eichlseder, Contribution to the fatigue assessment of laser welded joints, *Procedia Engineering* 10 (2011) 1785–1790
8. J. Baumgartner, T. Bruder, H. Hanselka, Fatigue strength of laser beam welded automotive components made of thin steel sheets considering size effects, *International Journal of Fatigue* 34 (2012) 65–75
9. D. Frank, Fatigue strength assessment of laser stake-welded T-joints using local approaches, *International Journal of Fatigue* 73 (2015) 77–87
10. W. Fricke et al, Fatigue strength of laser-welded thin-plate ship structures based on nominal and structural hot-spot stress approach, *Ships and Offshore Structures*, Vol. 10, No. 1, 39–44, 2015
11. P. Gallo, H. Remes, J. Romanoff, Influence of crack tip plasticity on the slope of fatigue curves for laser stake-welded T-joints loaded under tension and bending, *International Journal of Fatigue* 99 (2017) 125–136
12. M. Eib, C.M. Sonsino, H. Kaufmann, G. Zhang, Fatigue assessment of laser welded thin sheet aluminium, *International Journal of Fatigue* 25 (2003) 719–731
13. C. Hsu, C. Albright, Fatigue analysis of laser welded lap joints, *Engineering Fracture Mechanics* Vol. 39, No. 3, pp. 575-580, 1991

14. P.C. Wang, Fracture mechanics parameter for the fatigue resistance of laser welds, *International Journal of Fatigue*, Vol. 17, No.1, pp. 25-34, 1995
15. J. Willenborg, R. Engle and H. Wood, "A crack growth retardation model using an effective stress concept," AFFDL-TM-71-1-FBR, 1971
16. M. Ono, M. Kabasawa, M. Omura, Static and fatigue strength of laser-welded lap joints in thin steel sheet, *Welding International* 1997 II (6) 462-467
17. K. Sripichai, K. Asim, J. Pan, Stress intensity factor solutions for estimation of fatigue lives of laser welds in lap-shear specimens, *Engineering Fracture Mechanics* 78 (2011) 1424–1440
18. K. Asim, J. Lee, J. Pan, Failure mode of laser welds in lap-shear specimens of high strength low alloy (HSLA) steel sheets, *Fatigue Fract Engg Mater Struct* 35, 219–237, 2012
19. A.H. Noroozi, G. Glinka, S. Lambert, A study of the stress ratio effects on fatigue crack growth using the unified two-parameters fatigue crack growth driving force, *Int. J. Fatigue* 29 (2007) 1616-1634
20. S. Mikheevskiy, G. Glinka, T. Cordes, Total life approach for fatigue life estimation of welded structures, 3rd International Conference on Material and Component Performance under Variable Amplitude Loading, VAL2015, *Procedia Engineering* 101 (2015) 177 – 184
21. S. Bogdanov and G. Glinka, The Fatigue Life Prediction Methodology Based on the Unigrow Model, *Proceedings of ASME 2015 International Mechanical Engineering Congress & Exposition IMECE 2015-53693*, November 13-19, 2015, Houston, Texas, USA
22. R.Goyal, G.Glinka, Fracture mechanics based estimation of fatigue lives of welded joints, *Welding in the World*, September 2013, Volume 57, Issue 5, pp 625–634
23. M. Dourado et. al, A comparative study of fatigue behavior of MAG and laser welded components using reliability analysis, *Materials Science & Engineering A606* (2014) 31–39
24. S. Mikheevskiy, G. Glinka, "Elastic plastic fatigue crack growth analysis under variable amplitude loading spectra," *International Journal of Fatigue*, vol. 31, no. 11-12, pp. 1828-1836, 2009
25. O. Wheeler, "Spectrum Loading and crack growth," *J. Basic Engineering*, vol. 94, p. 181, 1972
26. J. Newman, "FASTRAN-2: A Fatigue Crack Growth Structural Analysis Program," 1992
27. S. Bogdanov, *Fatigue Life Prediction Based on the Advanced Fatigue Crack Growth Model and the Monte-Carlo Simulation Method*, Waterloo, ON, 2015
28. R. I. Stephens, S. G. Lee and H. Lee, "Constant and variable amplitude fatigue behavior and fracture of A572 steel at 25 C and -45 C," *International Journal of Fracture*, vol. 19, pp. 83-98, 1982
29. J. Yu and P. Ziehl, "Stable and unstable fatigue prediction for A572 structural steel using acoustic emission," *Journal of Constructional Steel Research*, vol. 77, pp. 173-179, 2012
30. H. F. Bueckner, "A novel principle for the computation of stress intensity factors," *Zeitschrift fuer Angewandte Mathematik & Mechanik*, vol. 50, no. 9, pp. 529-546, 1970

31. J. R. Rice, "Some remarks on elastic crack-tip stress fields," *International Journal of Solids and Structures*, vol. 8, no. 6, pp. 751-758, 1972
32. A. Seto, T. Yamamoto, T Niwa, Influences of loading direction and thickness ratio on fatigue properties of tailored welded blanks, *International Journal of Fatigue* 29 (2007) 729–737
33. P. Martinson, S. Daneshpour, M. Koçak, S. Riekehr, P. Staron, Residual stress analysis of laser spot welding of steel sheets, *Materials and Design* 30 (2009) 3351–3359
34. R. A. Sindhu, M. K. Park, S. J. Lee, K. D. LEE, Effect of residual stresses on the static and fatigue strength of laser welded lap joints with different welding speeds, *International Journal of Automotive Technology*, Vol. 11, No. 6, pp. 857–863 (2010)
35. Y.S. Yang, S.H. Lee, A study on the joining strength of laser spot welding for automotive applications, *Journal of Materials Processing Technology* 94 (1999) 151-156
36. S. K. Cho, Y. S. Yanga, K.J. Son, J.-Y. Kim, Fatigue strength in laser welding of the lap joint, *Finite Elements in Analysis and Design* 40 (2004) 1059–1070
37. K. Inosea, J. Y. Leeb, Y. Nakanishia, K. Y. Chul, Characteristics of welding distortion/residual stress generated by fillet welding with laser beam and verification of generality of its highly accurate prediction, *Welding International*, Vol. 23, No. 8, August 2009, 581–588
38. G. Labeas, I.Diamantakos, Laser beam welding residual stresses of cracked T-joints, *Theoretical and Applied Fracture Mechanics* 63–64 (2013) 69–76

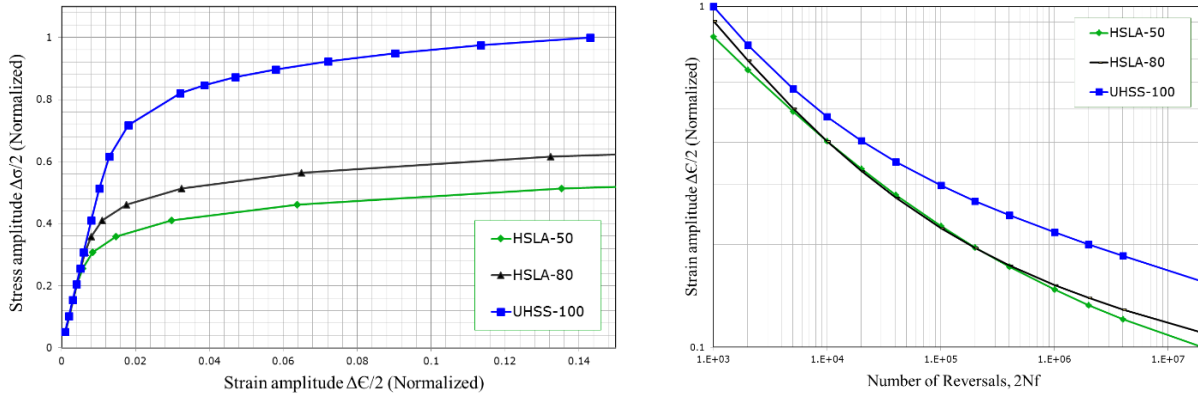


Fig. 1. Cyclic stress-strain (left) and strain life curves of 3 high strength steel materials selected for the study.

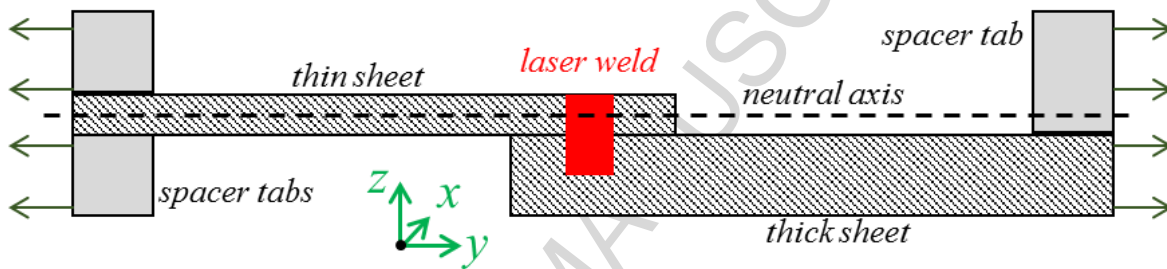


Fig. 2. Schematic diagram of a lap-shear joint with spacing tabs.

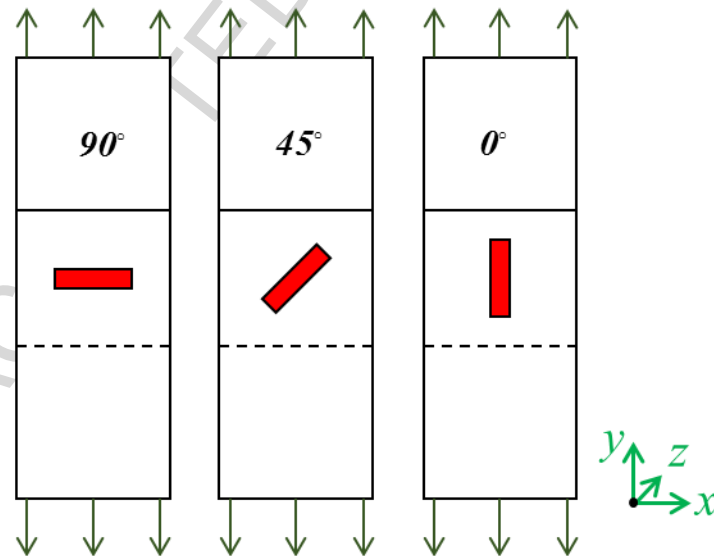


Fig. 3. The schematic representation of three orientations of laser welds with angles of 90° , 45° and 0° measured with respect to the applied load direction.

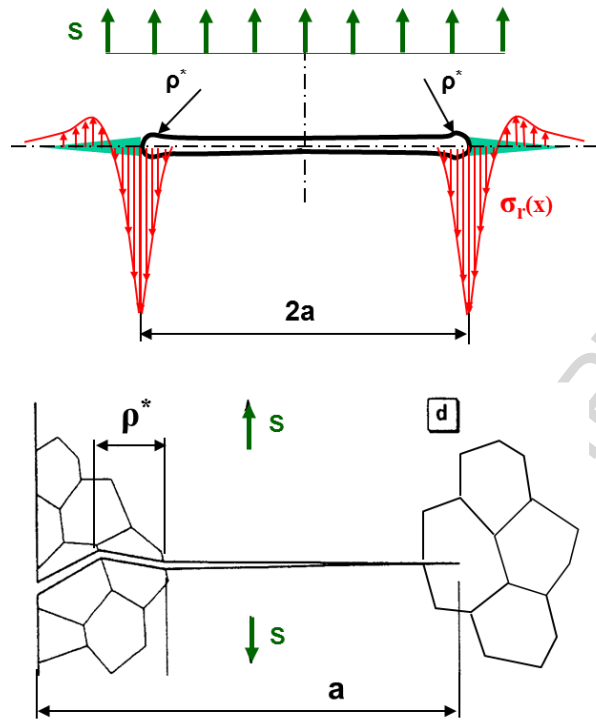


Fig. 4. Residual stress distribution, $\sigma_r(x)$ at the crack tip having the radius ρ^* (top) and the crack increment in the material composed of ρ^* elements/blocks [adapted from reference [19]].

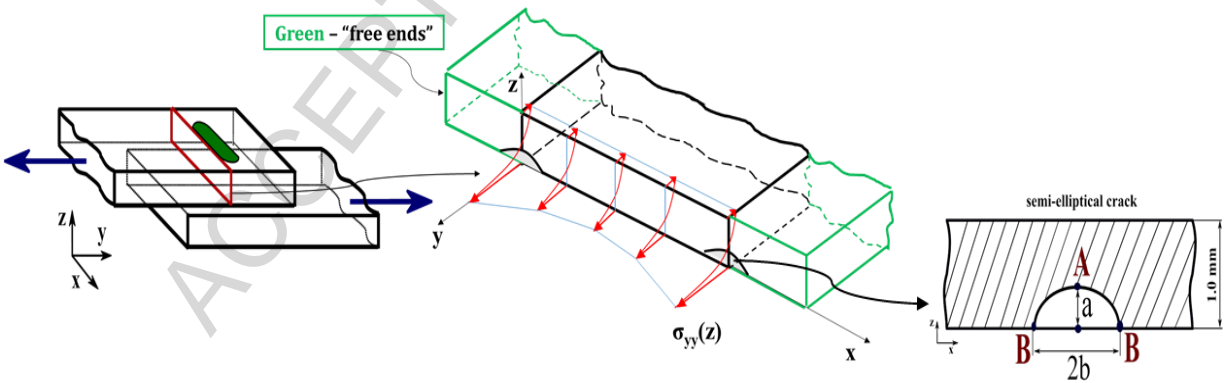


Fig. 5. Stress distribution over the critical crack plane at the weld root and the idealized semi-elliptical crack.

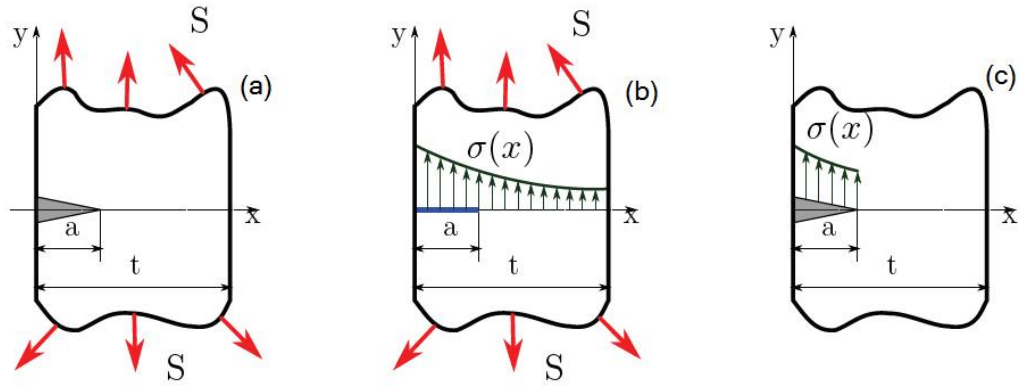


Fig. 6. The weight function method (a) cracked body with externally applied stress (b) geometrically identical body without crack (c) geometrically identical body with local stress applied to the crack faces.

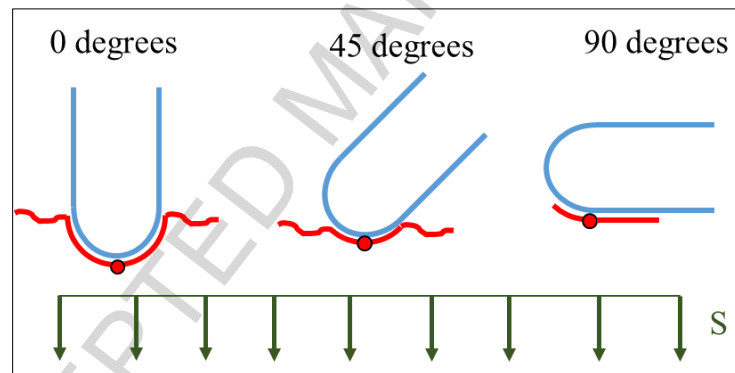


Fig. 7. Critical locations of fatigue cracks in various laser welded specimens.

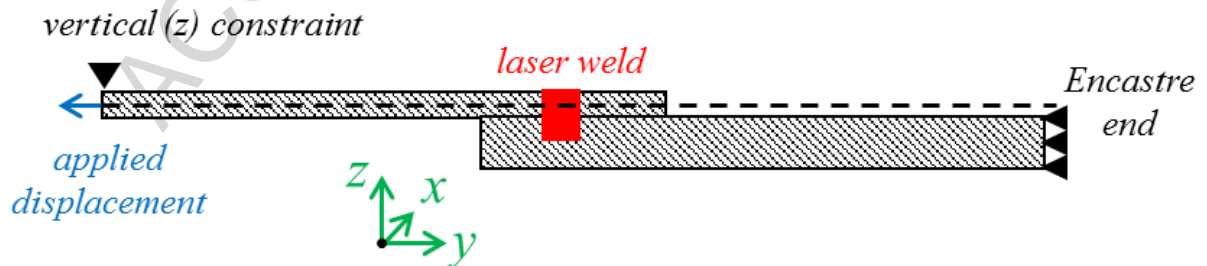


Fig. 8. Laser welded single lap joint with the applied displacement and boundary conditions.

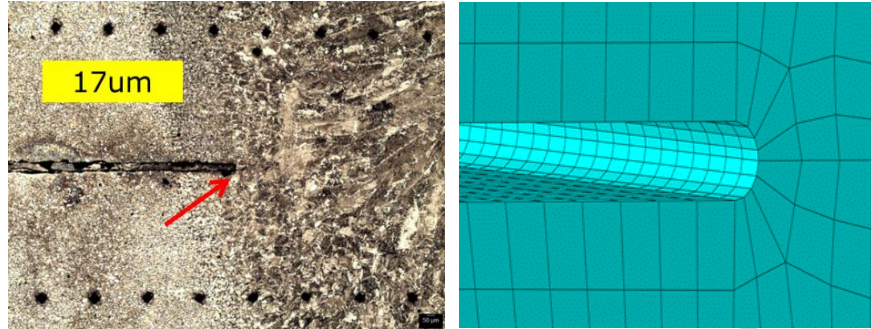


Fig. 9. The actual laser weld root radius visualized and measured (left) using metallography methods and the simulated one in the FE model (right) with 8 elements along the notch contour.

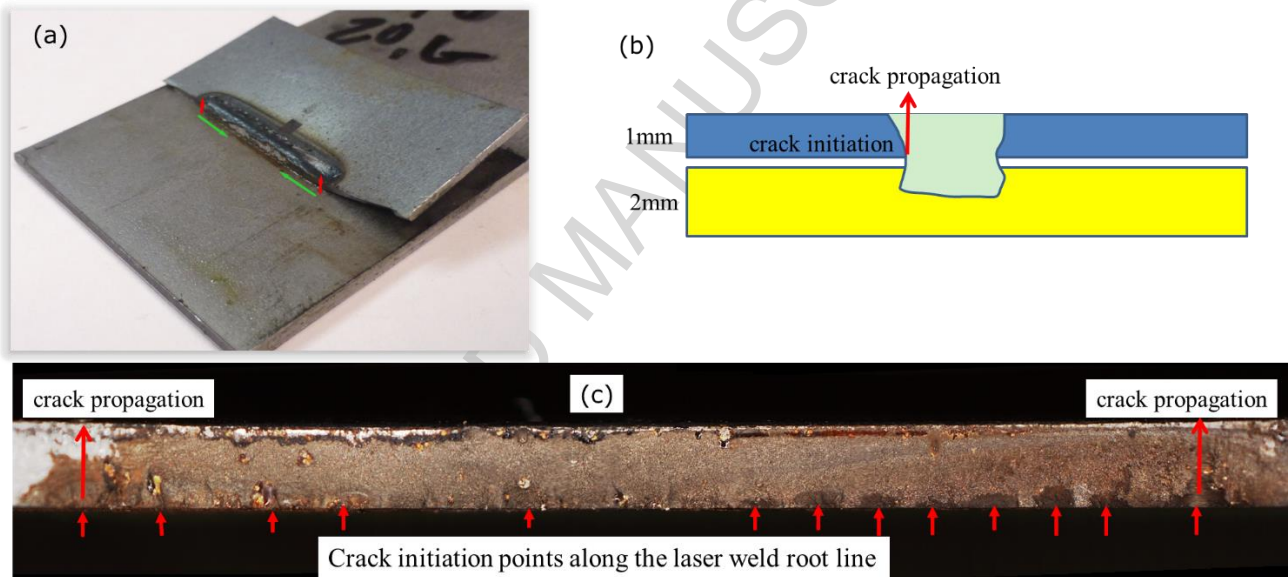


Fig. 10. Metallurgical evaluation showing (a) the fractured laser weld test sample with 90° weld orientation, (b) schematic sketch showing the crack initiation point and the direction of crack growth (c) Top plate sectional view of the crack plane with denoted multiple points of cracks initiation and propagation direction.

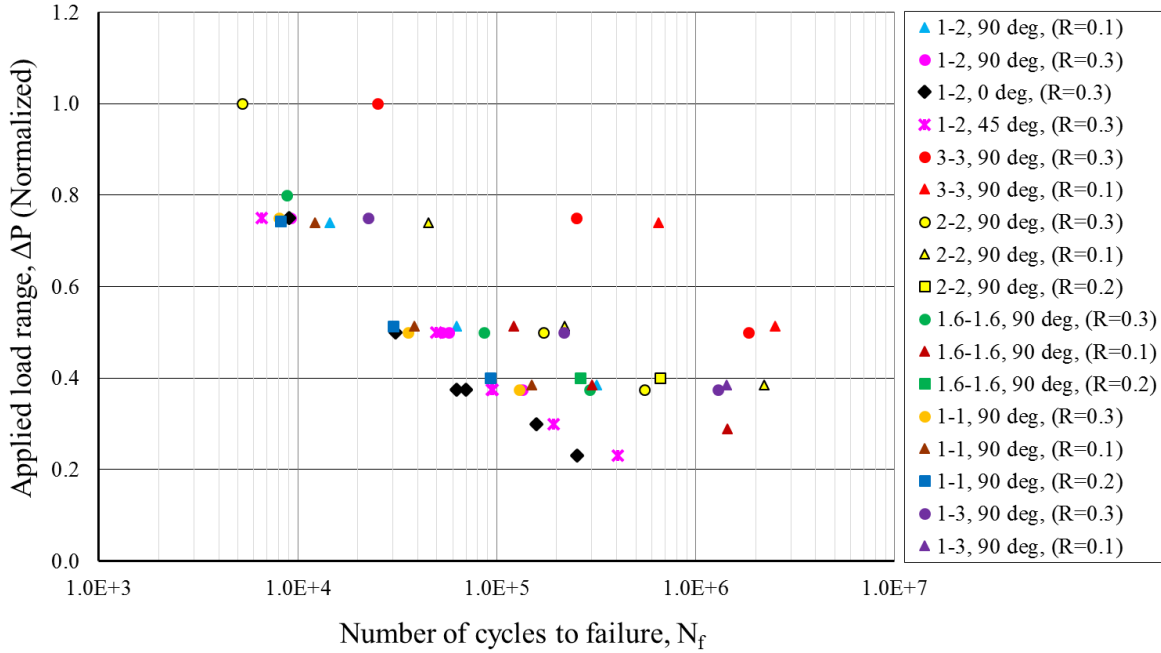


Fig. 11. Experimental fatigue lives obtained from fatigue testing of 56 laser welded joint samples.

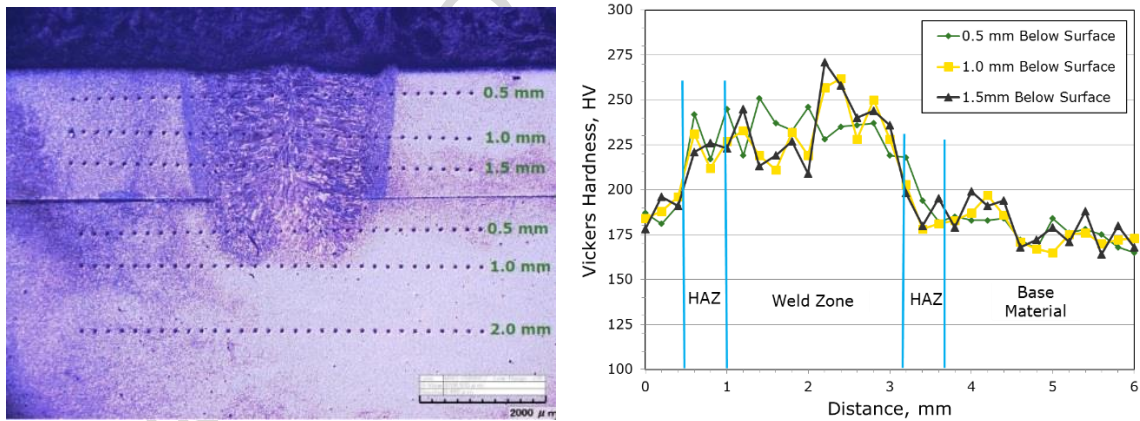


Fig. 12. Laser weld macro-graph (left) and variation of Vickers hardness (right) across the weld zone material, the HAZ (heat affected zone) and the base material (HSLA-50 steel material).

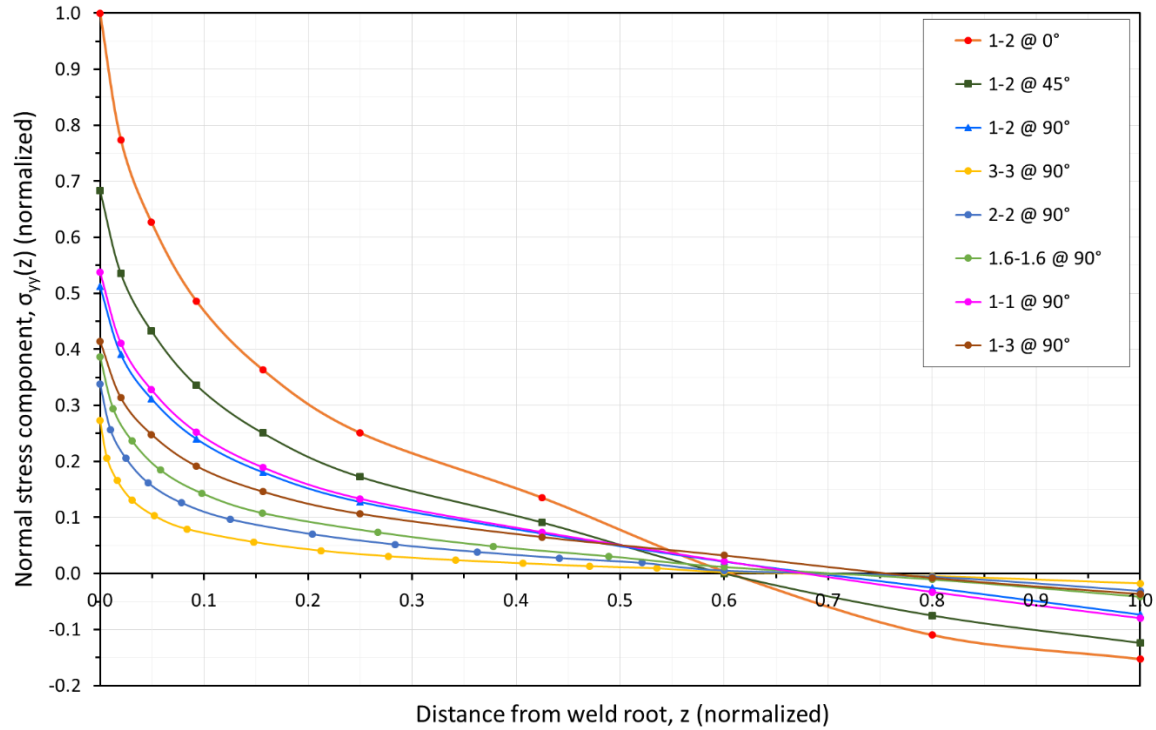


Fig. 13. Through-thickness stress distribution over the critical crack plane obtained from detailed 3D fine mesh FE analysis.

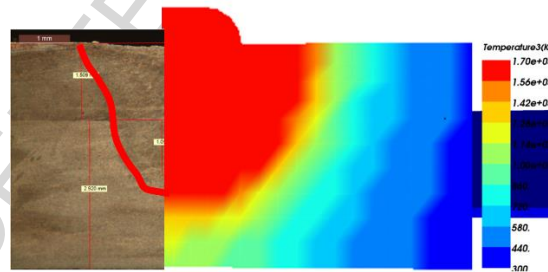


Fig. 14. Simulation results of the laser welding process showing the weld macrograph (left) and the matching simulated thermal profile (right).

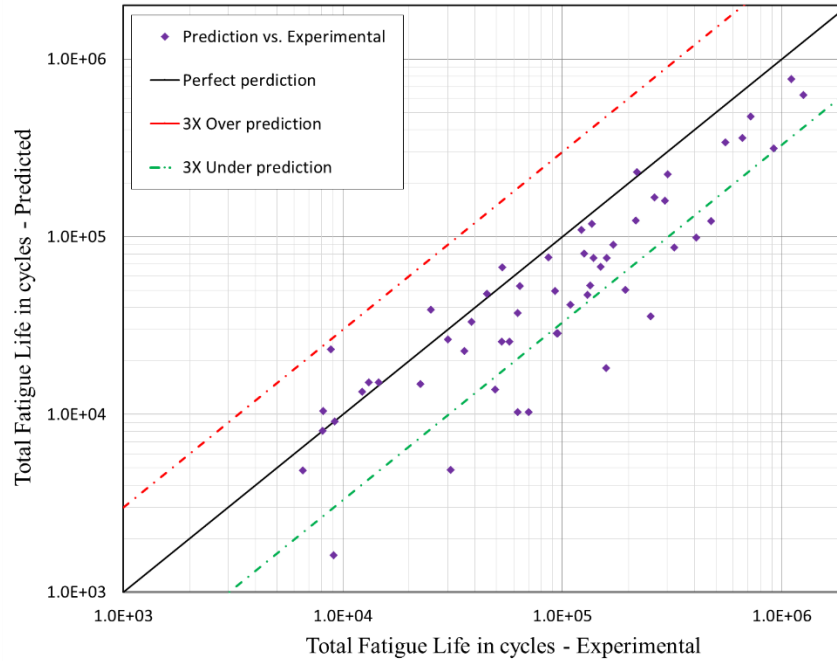


Fig. 15. Comparison of predicted total fatigue lives with the help of the UniGrow procedure (LEFM based) and corresponding experimental fatigue lives for all laser welded samples.

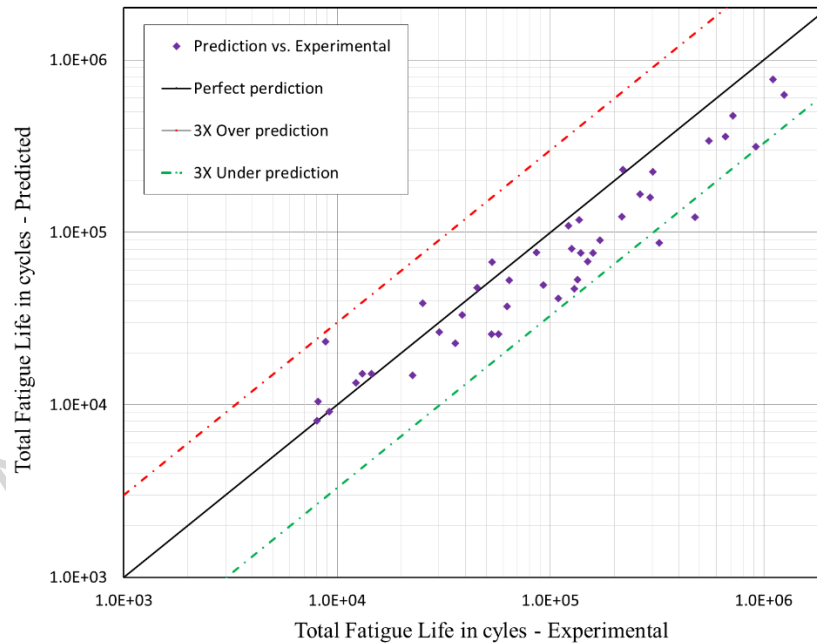


Fig. 16. Comparison of predicted, with the help of the UniGrow procedure (LEFM based), total fatigue lives and corresponding experimental fatigue lives of specimens with 90° weld orientation, i.e. excluded specimens with 0° and 45° weld orientation.

Table 1

Typical chemical composition high strength steel grades (wt. %) per ASTM A1011

Material	C	Mn	Si	P	S	Cr	Ni	Mo	Cu	V	Nb
HSLA-50	0.15	1.65	-	0.020	0.025	0.15	0.20	0.06	0.20	0.005	0.005
HSLA-80	0.15	1.65	-	0.020	0.025	0.15	0.20	0.16	0.20	0.005	0.005
UHSS-100	0.15	2.00	-	0.020	0.025	0.15	0.20	0.40	0.20	0.005	0.005

Table 2

Mechanical properties of high strength steel grades per ASTM A1011

Material	Yield Strength (MPa)	Tensile Strength (MPa)	Young's modulus (MPa)	Ultimate elongation (%)	Poisson's ratio
HSLA-50	340	410	210,000	22.0	0.29
HSLA-80	550	620	205,000	16.0	0.29
UHSS-100	690	760	209,000	12.0	0.29

Table 3

Summary of experimental tests and specimen data

Specimen ID	Number of specimens	Thick plate		Thin plate		Weld orientation	R-ratio
		Thickness (mm)	material	thickness (mm)	material		
1-2, 90°	7	2	HSLA-50	1	HSLA-80	90°	0.1, 0.3
1-2, 0°	7	2	HSLA-50	1	HSLA-80	0°	0.3
1-2, 45°	6	2	HSLA-50	1	HSLA-80	45°	0.3
3-3, 90°	5	3	UHSS-100	3	UHSS-100	90°	0.1, 0.3
2-2, 90°	9	2	UHSS-100	2	UHSS-100	90°	0.1, 0.2, 0.3
1.6-1.6, 90°	9	1.6	HSLA-80	1.6	HSLA-80	90°	0.1, 0.2, 0.3
1-1, 90°	9	1	HSLA-80	1	HSLA-80	90°	0.1, 0.2, 0.3
1-3, 90°	4	3	HSLA-50	1	HSLA-80	90°	0.1, 0.3

Table 4

Estimated fatigue crack growth properties of tested materials

	HSLA-50	HSLA-80	UHSS-100
Material block size ρ^* , m	3.9e-05	3.9e-05	3.9e-05
Elastic FCG coefficient C_{el}	6.48E-21	1.763e-24	4.451e-19
Elastic FCG exponent, γ_{el}	15.38	18.868	10.0
Plastic FCG coefficient C_{pl}	7.69E-12	8.893e-12	1.408e-11
Plastic FCG exponent, γ_{pl}	2.99	2.861	2.833

- Fatigue life estimation method of laser welded joints has been proposed.
- Fatigue test data for the laser welded joints of high strength steel thin sheets at 3 different R-ratios.
- Failure mechanism of laser welded joints under cyclic loading has been found.
- The UniGrow fatigue crack growth model based on total fatigue life approach has been utilized.
- Reasonable correlation with the experimentally obtained fatigue life test data has been shown.

ACCEPTED MANUSCRIPT

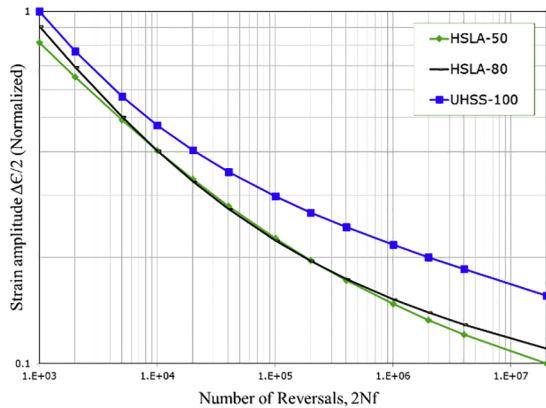
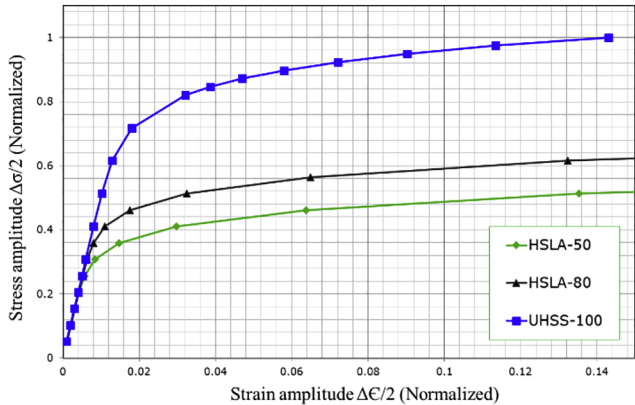


Figure 1

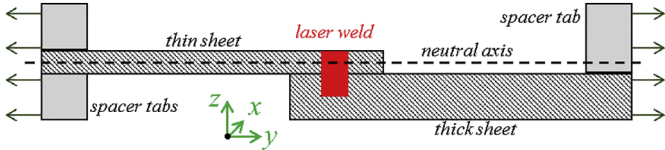


Figure 2

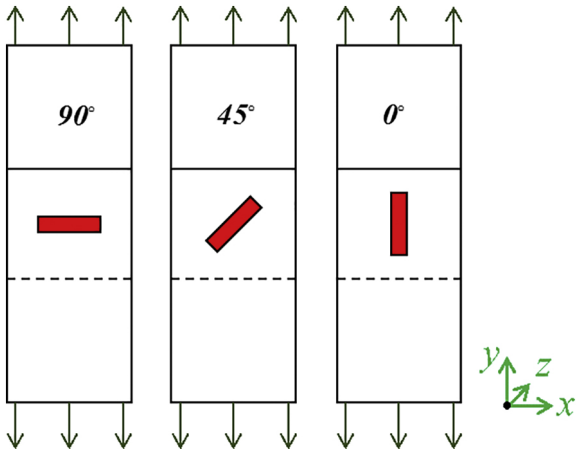


Figure 3

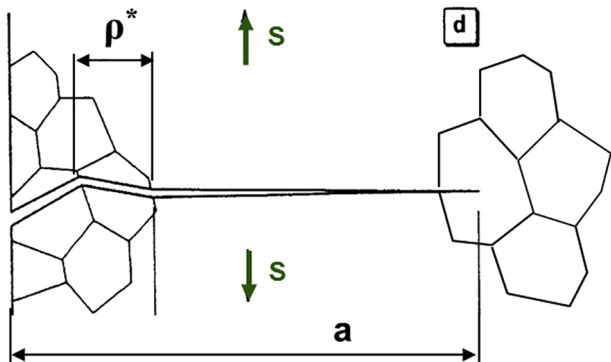
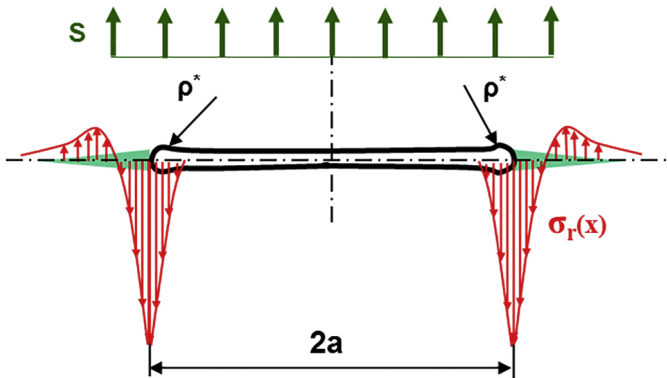


Figure 4

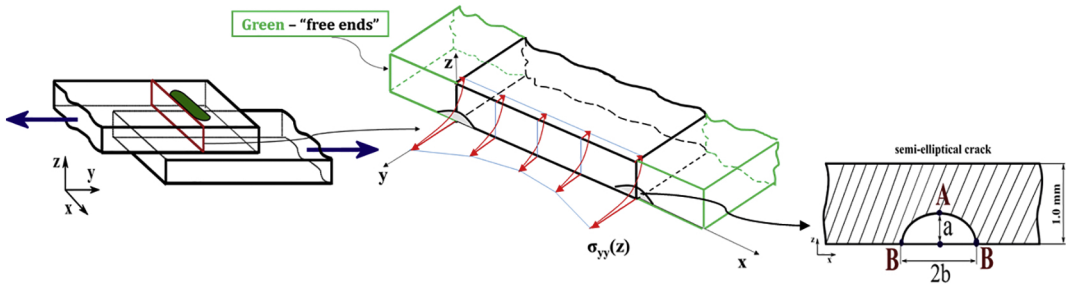


Figure 5

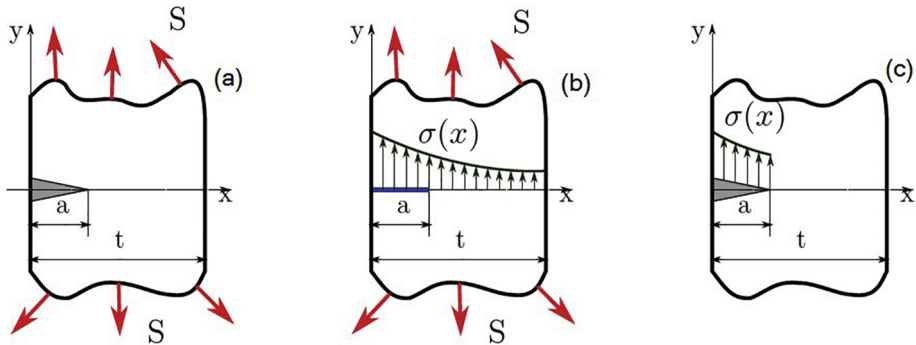
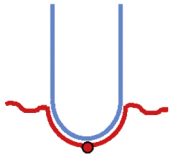
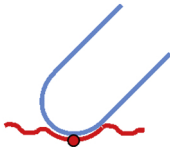


Figure 6

0 degrees



45 degrees



90 degrees

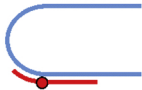


Figure 7

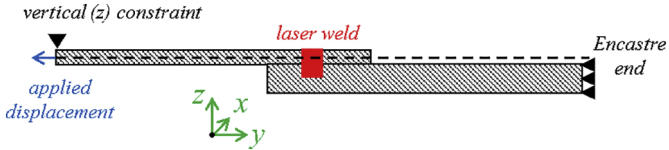


Figure 8

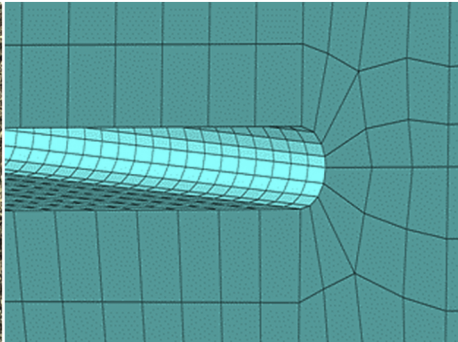
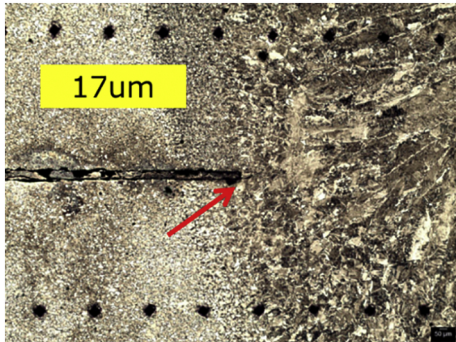


Figure 9

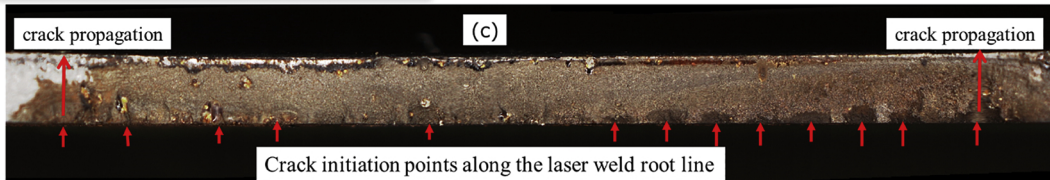
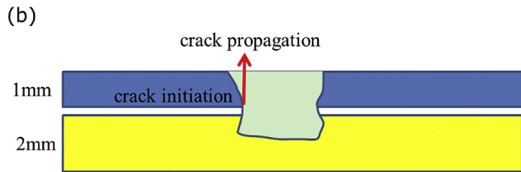
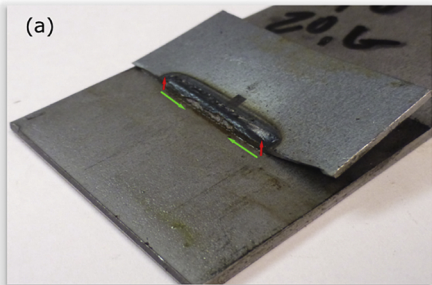


Figure 10

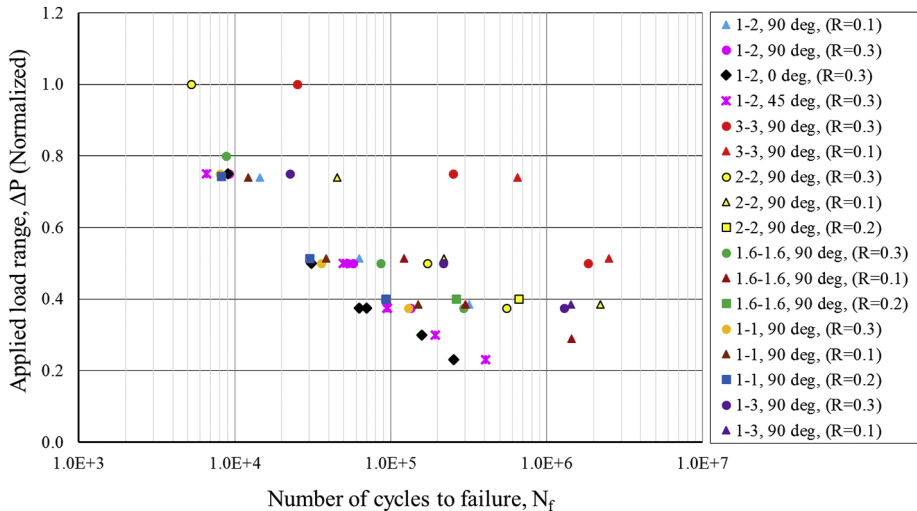


Figure 11

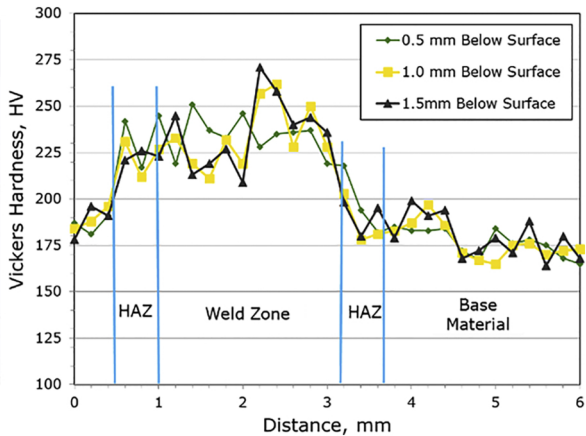
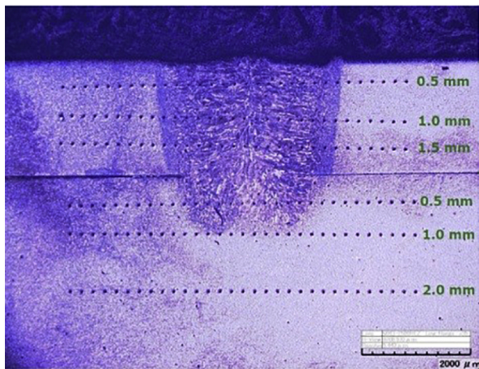


Figure 12

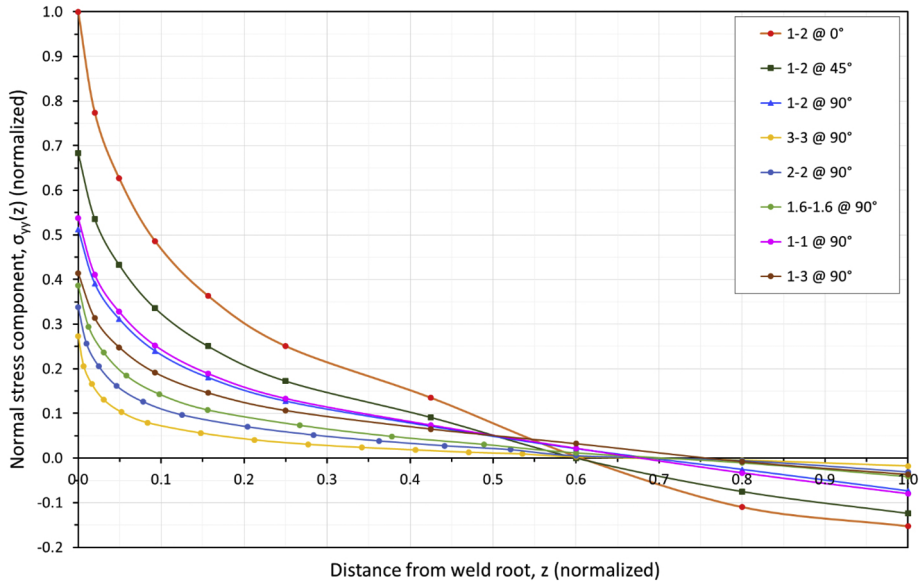


Figure 13

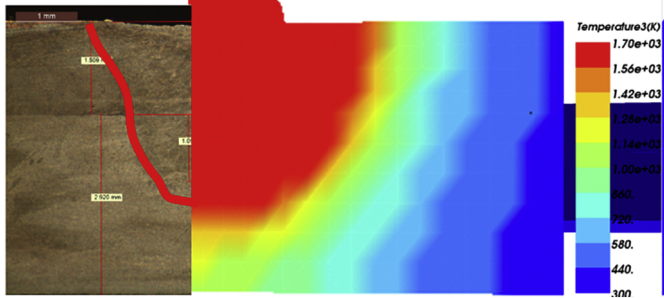


Figure 14

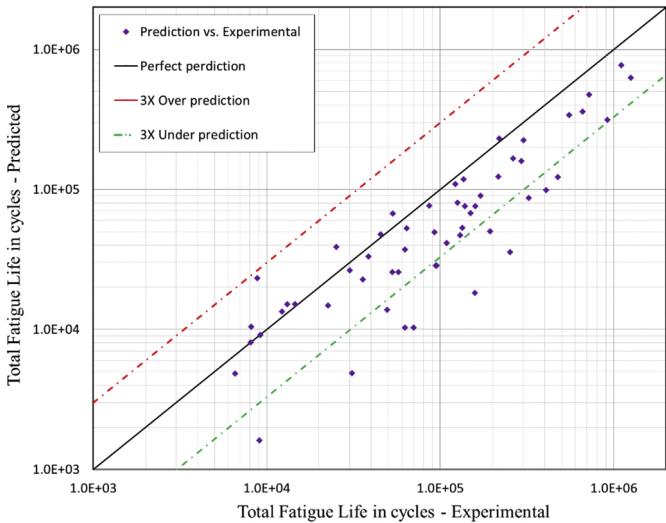


Figure 15

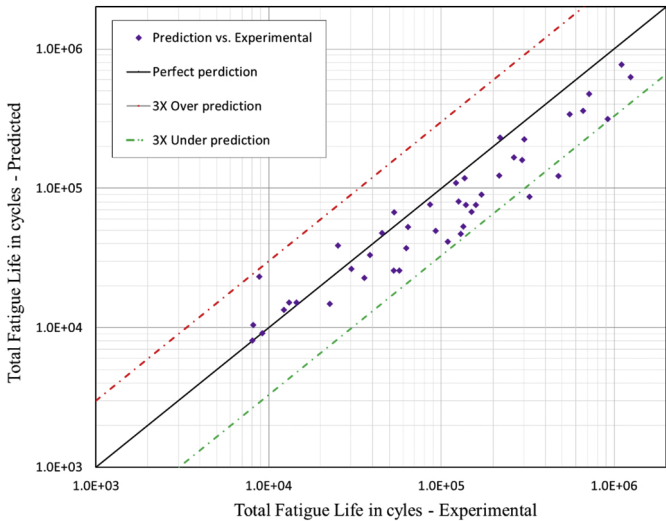


Figure 16